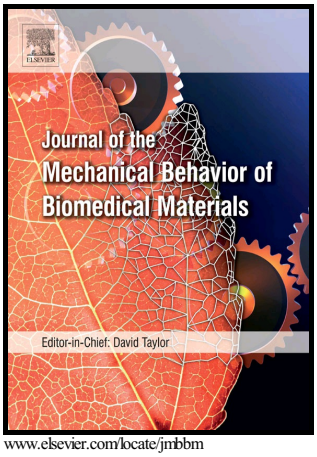

www.elsevier.com/locate/jmbbm

"Force-from-lipids" gating of mechanosensitive channels modulated by PUFAs

Pietro Ridone, Stephan L. Grage, Amrutha Patkunarajah, Andrew R. Battle, Anne S. Ulrich, Boris Martinac

PII: S1751-6161(17)30571-4
DOI: https://doi.org/10.1016/j.jmbbm.2017.12.026
Reference: JMBBM2629

To appear in: *Journal of the Mechanical Behavior of Biomedical Materials*

Received date: 22 October 2017
Revised date: 20 December 2017
Accepted date: 22 December 2017

Cite this article as: Pietro Ridone, Stephan L. Grage, Amrutha Patkunarajah, Andrew R. Battle, Anne S. Ulrich and Boris Martinac, "Force-from-lipids" gating of mechanosensitive channels modulated by PUFAs, *Journal of the Mechanical Behavior of Biomedical Materials,* https://doi.org/10.1016/j.jmbbm.2017.12.026

"Force-from-lipids" gating of mechanosensitive channels modulated by PUFAs

Pietro Ridone[a1], Stephan L. Grage[e,1], Amrutha Patkunarajah[d], Andrew R. Battle[c], Anne S. Ulrich[e], Boris Martinac[a,b*]

[a]Victor Chang Cardiac Research Institute, Darlinghurst, NSW 2010, Australia,

[b]St Vincent's Clinical School, University of New South Wales, Darlinghurst, NSW 2010, Australia,

[c]Translational Research Institute (TRI) and Institute of Health and Biomedical Innovation (IHBI), School of Biomedical Sciences, Queensland University of Technology (QUT), Brisbane, QLD 4000, Australia,

[d]School of Medical Sciences , University of New South Wales, Kensington, Sydney 2052, Australia,

[e]Institute for Biological Interfaces IBG-2, Karlsruhe Institute of Technology, Karlsruhe, Germany

***Corresponding author:** Boris Martinac. Victor Chang Cardiac Research Institute, 405 Liverpool St, Darlinghurst, NSW 2010, Australia

ABSTRACT

The level of fatty acid saturation in phospholipids is a crucial determinant of the biophysical properties of the lipid bilayer. Integral membrane proteins are sensitive to changes of their bilayer environment such that their activities and localization can be profoundly affected. When incorporated into phospholipids of mammalian cells, poly-unsaturated fatty acids (PUFAs) determine the mechanical properties of the bilayer thereby affecting several membrane-associated functions such as endo- and exo-cytosis and ion channel/membrane receptor signalling cascades. In order to understand how membrane tension is propagated through poly-

[1] These authors have equally contributed to this work.

unsaturated bilayers, we characterized the effect of lipid saturation on liposome reconstituted MscS and MscL, the two bacterial mechanosensitive ion channels that have for many years served as models of ion- channel-mediated mechanotransduction. The combination of NMR and patch clamp experiments in this study demonstrate that bilayer thinning is the main responsible factor for the modulation of the MscL threshold of activation while a change in transbilayer pressure profile is indicated as the main factor behind the observed modulation of the MscS kinetics. Together, our data offer a novel insight into how the structural shape differences between the two types of mechanosensitive channels determine their differential modulation by poly-unsaturated phospholipids and thus lay the foundation for future functional studies of eukaryotic ion channels involved in the physiology of mechanosensory transduction processes in mammalian cells.

Graphical abstract

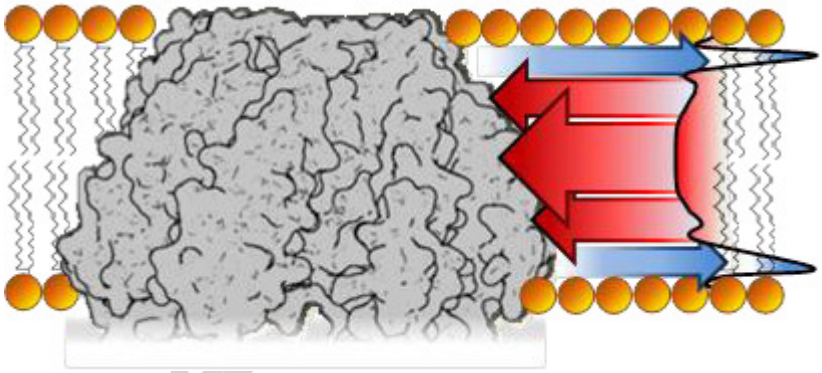

LIST OF ABBREVIATIONS

MscS, Mechanosensitive channel of Small conductance; MscL, Mechanosensitive channel of Large conductance; TRPC1, Transient Receptor Potential Channel 1; GPCR, G-Protein Coupled Receptor; NMR, Nuclear Magnetic Resonance; WT, Wild-Type; PUFA, Poly-Unsaturated Fatty Acid; PE, Phosphatidyl-Ethanolamine; PC, Phosphatidyl-Choline; DOPE, Di-Oleyl Phosphatidyl-Ethanolamine; DOPC, Di-Oleyl Phosphatidyl-Choline

Keywords: MscL, MscS, patch clamp, NMR, liposomes, transbilayer pressure profile

INTRODUCTION

It is increasingly evident that the function of integral membrane proteins is coupled to the mechanical properties of their membrane lipid environment [1]. Changes in the mechanical properties of the lipid bilayer are associated with a variety of disease states including diabetes, obesity, hypertension, cancer, and neurological and heart diseases [2]. Biophysical parameters of the lipid bilayer such as hydrophobic thickness, elastic and bending moduli and transbilayer pressure profile determine the energetic thresholds for conformational transitions, quaternary structure and localization of membrane proteins [3]. Furthermore, many members of major ion channel families have been shown to be affected by partitioning into cholesterol-rich membrane domains [4]. A number of mechanosensitive (MS) ion channels in eukaryotes have also been found to associate with cholesterol-binding proteins as reported for MEC-4 and MEC-10/MEC-2, Piezo1 and Piezo2/STOML3 and TRPC6/Podosin, as cholesterol is thought to suppress mechanical noise in lipid rafts [5], and thus ensure proper mechanosensitive response [6]. Phospholipids containing PUFAs have been shown to affect the distribution and cholesterol content of lipid rafts [7] as well as to enhance allodynia in *C. elegans* [8]. Treatment of human endothelial cells with DHA (Docosahexaenoic acid), and its consequent incorporation in phospholipids, resulted in displacement of TRPC1 from caveolar lipid rafts and suppression of calcium currents [9]. Other, apparently unrelated, physiological processes like photomechanical response [10] and unfolded protein response (UPR) from the ER (endoplasmic reticulum) membrane [11] have been shown to be affected by changes in lipid saturation of their respective membranes. The role of PUFAs in GPCR regulation (eg. bovine rhodopsin) by the lipid bilayer

has also been investigated [12]. In addition, membrane fluidity in macrophages is determinant for phagocytotic efficiency [13]. The emerging picture makes control of the membrane biophysical parameters, including PUFAs, an attractive therapeutic strategy for a vast number of cardiovascular [14], [15], neurological [16],[17],[18],[19], metabolic diseases [11], [20] and cancers [7], [21]. We hypothesize that many of the above-mentioned processes fundamentally depend on modulation of the "force-from-lipids" experienced by the critical membrane proteins driving the progression of the disease.

In this study we have characterized the contribution of PUFAs to mechanotransduction of *E. coli* MscS and MscL channels reconstituted into liposomes. Using these bacterial MS channels we investigated by the patch clamp technique how mechanical force transmitted via homogeneous mono- and polyunsaturated PE/PC bilayers might affect their gating mechanism to complement our previous [22] and complete our current studies of differential effects of various types of lipids on these model channels of the MS channel activation by bilayer tension. To understand better our patch clamp results we also studied different mechanical environments within the unsaturated bilayers using NMR spectroscopy. The determination of the lipid order parameters allowed us to estimate the bilayer thicknesses of the PE/PC bilayers, which enabled us further to generate a map of the corresponding transbilayer pressure profiles of the hydrophobic core of the bulk bilayer at the single C-C bond resolution (**Fig. 1**). To our knowledge, this has been done for the first time for polyunsaturated lipid bilayers in this study. The combination of the two complementary experimental approaches enabled us to successfully interpret the observed MS channel gating behavior in relation to stress/pressure distributions within the lipid bilayer, which

according to the "force-from-lipids" principle affect structural changes between the closed and open channel conformations and consequently, the gating kinetics of MscL and MscS [23],[24].

MATERIALS AND METHODS

Protein purification

WT MscL and WT MscS proteins were purified as previously reported [22]. The MscL gene fused to N-terminal 6x His-tag (pQE-32 vector), and the MscS gene, fused to the C-terminal 6x His-tag (pQE-60 vector), were expressed in M15 *E. coli* competent cells containing pREP4 (Qiagen) and pRARE (Merck). Cells were cultured in LB medium at 37 °C until OD600 = 1.0 with the appropriate antibiotic (ampicillin 100 μg/mL, kanamycin 12.5 μg/ml, and chloramphenicol 12.5 μg/mL). Expression was induced with 0.8 mM IPTG in the presence of 0.4 % glycerol for 4 h at 25 °C. Protein purification was achieved by affinity chromatography on TALON Co^{2+} Sepharose column (Clontech, Mountain View, CA, USA).

Liposome preparation

The dehydration/rehydration (D/R) method was performed as reported in previous studies [25, 26]. DOPC (18:1, 850375P, Avanti), DOPE (18:1, 850725P, Avanti), PC 18:2 (850385P, Avanti), PE 18:2 (350755C, Avanti), PC 18:3 (850395P, Avanti), PE 18:3 (850795C, Avanti) were used for the liposome preparation. All buffers were bubbled in N_2 gas for at least 1 hr before preparation. MscS and MscL proteins were reconstituted into bilayers at 1:200 and 1:1500 protein-to-lipid ratio (weight:weight) respectively. Rehydration of 18:2 and 18:3 samples was performed with dried lipids and buffers at room temperature.

Electrophysiology

All recordings were performed in symmetrical bath and pipette solution containing 200 mM KCl, 40 mM $MgCl_2$, 5 mM HEPES (solution adjusted to pH 7.2 using KOH). The recording solution was bubbled in N_2 gas for at least 1 hr before patch clamp recording. Borosilicate glass pipettes (Drummond Scientific, Broomall, PA) were pulled using a Narishige puller (PP-83; Narishige) to achieve a bubble number of 6.0 (3 – 4 MΩ pipette resistance). The channel currents were recorded with an AxoPatch 1D amplifier (Axon Instruments) in the inside-out patch configuration, and data were taken at 5-kHz sampling rate with 2-kHz filtration. Suction was applied to the patch membrane using a computer-controlled high-speed pressure clamp-1 apparatus (HSPC-1; ALA Scientific Instruments).

For mono-reconstituted channels, we averaged data from at least 4 consecutive pressure ramps on the same patch. These mean values were then averaged over n different patches. The n values for Fig. 2D are as follows: MscS in 18:1 (n=7), MscS in 18:3 (n=3), MscL in 18:1 (n=7), MscL in 18:3 (n=5).

The data of the co-reconstituted samples (**Fig. 2E**) was treated in the same way as for mono-reconstituted samples. The pressure values obtained from consecutive pressure ramps on the same patch were averaged together. These mean values were then averaged over n different patches. Thus, each n represents a different patch. The n values are as follows: 18:1 lipid (n=31), 18:2 (n=8), 18:3 (n=26). A Boltzmann function ($f(P) = \frac{Imax}{1+e\text{^}[\frac{Pmid-P}{Pc}]} + C$) was fitted to Current (I) vs Pressure (P) traces to estimate the sensitivity of MscS and MscL (**Figs. 2F, 2G, 2H, 2I**). These were plotted using data collected from co-reconstituted samples. Only traces where the current from both channel species reached saturation (I_{max}) were analyzed. The following values

indicate 18:1/ 18:2/ 18:3 lipid, respectively: n values for Fig. 2F are 8 / 3 / 5; n values for Fig. 2G are 7 / 7 / 7; n values for Fig. 2H are 12 / 5 / 4; n values for Fig. 2I are 6 / 4 / 6.

The patch clamp recordings were analyzed using the Single-Channel Search analysis tool of Clampfit as previously described [26] by applying the threshold crossing method [27]. The event threshold was arbitrarily set to 95% to recognize complete gating events during HSPC1-controlled 4-s ascending and 4-s descending ramp protocols applied to inside-out patches of mono- and co-reconstituted MscS and MscL. One 'event' was defined as a single closed-to-open or open-to-closed transition for an MscS channel: for example, one full gating cycle of MscS produced two distinct events representative of two distinct motions (opening and closing) exhibited by the single ion channel protein. Data for 18:1 and 18:2 samples was collected from randomly chosen traces from different patches containing at least 20 MscS channels. Data for 18:3 samples was instead gathered from traces with at least 10 MscS channels. All the analyzed traces were collected from mono-reconstituted samples. Student's t-test was used to calculate the p-value of the observed difference in Events/MscS between 18:1 (n=7), 18:2 (n=4) and 18:3 (n=16) samples.

NMR experiments

Sample preparation (18:1/2/3 lipids) and data collection were done as follows. ^{1}H-^{13}C dipolar couplings were measured of six oriented bilayer samples of PC-lipids and a mixture of PC:PE lipids (molar ratio 2:1) lipids, with 18:1, 18:2 and 18:3 chains. (Note, that less PE lipids were used in the mixtures of PC and PE lipids in the NMR experiment as compared to the patch

clamp experiments due to the longer duration of the NMR experiments and faster degradation of the polyunsaturated PE lipids.) Oriented samples were prepared by dissolving 10-20mg lipids in chloroform, spreading the solution on ~15 glass slides (7.5 x 12 x 0.06 mm), evaporating the solvent under nitrogen and drying under vacuum. The slides were stacked and sealed in a glass container together with wet tissue providing water for hydration, and incubated for > 3h at room temperature. SAMPI4 separated local field spectra [28] with ^{1}H and ^{13}C radiofrequency amplitudes of 40 kHz were collected at 25°C using a double resonance probe equipped with a flat coil on a Bruker A vance III spectrometer operating at a ^{1}H resonance frequency of 500 MHz. The resonances were assigned and dipolar couplings processed further as described in more detail in the Supplementary Material.

Acyl chain parameters and lateral pressure calculation

Order parameters were determined as the ratio of the observed ^{1}H-^{13}C dipolar coupling (reduced by motion and dependent on the segment alignment), and the maximally possible value. The contribution of each chain segment to the bilayer thickness and the lateral pressure profile were deduced from these order parameters as described in the Supplementary Material. The analysis is based on assuming discrete possibilities for the torsion angles along the chain. For each resulting segment conformer, the segment thickness and order parameter contribution can be calculated from simple geometrical considerations. The averages of the order parameter contributions over all conformers of a segment were set equal to the measured order parameters. The respective average of the segment length was derived as a function of the average order parameters of the considered segment. For saturated chain stretches, the conformations were assumed according to the diamond lattice model [29]. This model allows to relate the average segment thickness to the

average order parameter without knowledge of the individual probabilities of each conformer: $<D_k> = D_b (2/3)1/2 (1/2-<S_{CH,k}>)$, where D_b is the C-C bond length. For the unsaturated CH_2-CH=CH-CH_2 segments, a plausible, reduced set of conformers was used which allowed deriving a similar relationship: $<D_k> = (D_b + D_{bb}) (-0.283 <S_{CH1,k}> + 0.102 <S_{CH2,k}> + 0.389$, where D_b and D_{bb} are the C-C and C=C bond lengths, $<S_{CH1,k}>$ and $<S_{CH2,k}>$ are the order parameters of the C-H bonds adjacent to the double bond.

The lateral pressure values where estimated from the pressure p_k needed to compress the segment volume from its unconstrained value V_0 (27.6 $Å^3$ for CH_2-groups) to the volume VM = AS <Dk> corresponding to the measured segment thickness: $p_k = K_V \ln(A_S <D_k> /V_0)$. The area A_S of each segment was calculated as the surface area per lipid from the order parameters of the plateau region following previous reports [29, 30]. For these considerations, the bulk compressibility modulus K_V was derived from the area compressibility modulus K_A as $K_V = K_A / (2 D_C)$, where 2 D_C is the thickness of the acyl chain region. Values for K_A were obtained from [31].

RESULTS

Electrophysiology

We have reconstituted WT MscS and WT MscL purified from *E. coli* cells, separately (**Fig. 2A** and **Fig. 2B**) and together (**Fig. 2C**) in liposomes made of 70% Phosphatidyl-ethanolamine (PE) and 30% Phosphatidyl-choline (PC) using the Dehydration/Rehydration method, as previously

described [32],[25]. The level of saturation of PE and PC was kept identical in each sample, in order to produce uniform 18:1, 18:2 and 18:3 bilayers. To ensure this, we prepared 18:2 and 18:3 samples using Dehydration/Rehydration (DR) buffer (200mM KCl, 40mM $MgCl_2$, 5mM HEPES) gassed and saturated with nitrogen (N_2), to minimize lipid oxidation throughout the protocol. Likewise, all recording solutions used in the patch clamp experiments were saturated with N_2 before recording. Liposomes were patched in the inside-out excised patch configuration under control of a high-speed-pressure-clamp (HSPC) device generating a triangular pressure pulse characterized by an increasing pressure ramp followed by a decreasing ramp, each 4 s long, as previously described [26]. The maximal pressure, and hence the rate, was changed during the experiments to either saturate MscL currents or prevent the patch from breaking, given the lower lytic pressure observed in 18:2 and 18:3 bilayers (data not shown). We recorded the pressure at which we could detect the first opening and the last closing event for both MscS and MscL, as indicated by the arrows in **Fig. 2C**. These results are quantified in **Fig.2D**, for mono-reconstituted samples (either MscS- or MscL-containing liposomes), and **Fig.2E**, for co-reconstituted samples (liposomes containing both MS channels). Our results show that poly-unsaturated lipids cause MscL to activate at lower pressures with respect to mono-unsaturated lipids (**Fig. 2B, 2C**) while MscS channel closing is significantly delayed in poly-unsaturated lipids (**Fig. 2A, 2C**). The overall sensitivity of both MS channel populations in these different lipid environments was estimated by analyzing the Boltzmann relationship between current (I) and pressure (P) (see Methods section). Our results show again that all MscL channels in the patch become more sensitive with increasing lipid unsaturation, during both the activation and closing regimes (Fig.2F and 2G), while MscS channels are unaffected in their activation phase but close at lower pressures in poly-unsaturated lipids (Fig.2H and 2I) reflecting a remarkable

increase in the hysteresis of MscS and stabilization of its open state. In addition, we have observed a dramatic decrease in the number of open-to-closed transitions in McsS during our ramp experiments with 18:3 bilayers (**Fig. 3**), which was coupled with increasing MscS hysteresis. These results share resemblance with our previous study in which we have shown that MscS hysteresis and fast kinetics characterized by very short channel openings can be oppositely modulated by cardiolipin in azolectin liposomes [26]. **Fig. 2A** and **Fig. 3A**, **3B** and **3C** are examples showing how MscS kinetics can further be modulated by its lipid environment depending on the saturation of the fatty acids of the phospholipid molecules constituting the lipid bilayer.

NMR experiments

The transbilayer pressure distribution within the unsaturated bilayers used in this study and their geometrical parameters were addressed using natural abundance $^{13}C/^{1}H$ solid-state NMR on oriented samples. By measuring ^{13}C-^{1}H dipolar couplings of 18:1, 18:2 and 18:3 chains using separated local field experiments, we obtained order parameter profiles of PC lipids (**Fig. 4A**) and 2:1 mixtures of PC/PE lipids (**Fig. 4B**). The order parameters reflect the local mobility within the chain, and are related to the distribution of conformations of the individual chain segments. A model for the conformations within unsaturated chains was developed (see **SI** for details), which allowed us to estimate the contributions of the individual chain segments to the bilayer thickness (**Fig. 4C, D, Table 1**). The thicknesses of each segment, z, related to the maximum possible thickness if the segment was extended along the membrane normal, z_{max}, are shown in Fig 4C,D as a function of the carbon position along the chain. The sum of all segment thicknesses yields the thickness of the hydrophobic core of the membrane, as summarized in

Table 1. The area per lipid (**Table 1**) was determined from the plateau region of the order parameter profile as described earlier [29],[33]. Assuming an area compressibility of ~250 mN/m [31], and the determined areas per lipid (**Table 1**), we were able to convert the vertical segment extensions to estimates of the pressure exerted by each carbon of the chain within the hydrophobic core of the bilayer (**Fig. 4C, D**). Our results show that the order parameter is reduced for the segments following each double bond (**Fig. 4A, B**). As the number of double bonds increases, the chain order is more and more decreased towards the end of the acylchains. In total, our study shows that the acyl chains are increasingly disordered as the chain unsaturation is increased, extending previous findings on lipids with a single unsaturated chain to lipids with two poly-unsaturated chains [34] [35]. Applying the configuration model (see SI), the segment thicknesses z/zmax (**Fig 4C,D**) follow a similar pattern as the order parameter, as the thickness contribution is reduced for the chain segments following each double bond. This leads to a reduction of the segment thicknesses towards the end of the acyl chains, which gets more pronounced with higher number of double bonds. Both, chain order and segment thickness influence then the local lateral pressure, defined as force per length, along the lipid chains (**Fig 4E,F**), where we found an increase in lateral pressure with higher degree of unsaturation for the center of the bilayer. In fact, if the membrane thickness of all three lipids bilayers were the same, the lateral pressure profile in all three cases would look very similar and differ mostly in its height (**Fig 4E, F**). Hence overall, the increase in chain disorder in the multiple unsaturated lipids results in increasing local transbilayer pressure values. At the same time, the membrane thickness is reduced with higher number of double bonds. Interestingly, the sum of the pressure across the entire bilayer (**Table 1**) does not vary too much, but increases only slightly from 11.5 mN/m to 14.0 mN/m in the case of PC, and is constant around 12 mN/m in the case of PC/PE

lipids. This way, the pressure distribution within the bilayer, rather than the total pressure, changes with saturation when considering both local pressure increase and membrane thinning together. In other words, a wide chain region of elevated lateral pressure in the case of 18:1 chains changes to a more compact region in the core of the bilayer of very high lateral pressure in the case of 18:3 lipids.

We note that, although the derived transbilayer pressure profile constitutes a semi-quantitative estimate the results are valid for several reasons: (i) they result in typical values for the integral parameters such as the hydrophobic bilayer thickness and the area per lipid, (ii) the trend of decreasing thickness and increasing area per lipid with increasing number of double-bonds is as expected, and (iii) the values for the transbilayer pressure integrated over the chain region are in the right order of magnitude and in agreement with literature values [36]. It is conceivable that the repulsive transbilayer pressure of the acyl chains of ~ 10-15 mN/m together with the (here not considered) pressure of the headgroups (of approximately equal size, see Marsh [37]), i.e., in total around 20-30 mN/m, balances the surface tension, for which values of ~35mN/m [37] and 50mN/m [38] have been reported. Moreover, there is little doubt that double bonds lead to an increased disorder (lower order parameters), readily understood by the increased number of conformers resulting from deviations from an all-trans saturated chain, as previously reported by numerous investigators, [34], [35], [36], [39], [40]. In a lipid with two unsaturated chains, the membrane thickness is determined by these unsaturated chains, and thinning effects are not limited by the presence of a stiffer saturated chain keeping the monolayers at a distance. For increased disorder and decreased thickness, an increase in lateral force is then expected, in accordance with our results.

DISCUSSION

The transbilayer pressure profile has been thus far a concept beyond direct experimental evidence despite that some attempts have been made to determine it [41], [42]. Most studies of transbilayer pressure profiles, in particular the profiles of unsaturated lipids, have been performed by atomistic MD simulations, due to the difficulties of assessing these parameters experimentally. The lateral pressure profiles derived this way give a controversial picture. Whilst some studies support the notion of increased transbilayer pressure in the center of the bilayer due to the presence of double-bonds [38],[43], Ollila et al, for example, demonstrated a decrease in lateral pressure in the bilayer center of poly-unsaturated acyl chains [44]. Most studies, however, considered lipids with only one unsaturated chain, resulting in different effect of the double bonds on membrane thickness. As the lateral pressure is a result of both segment thickness and order parameter, our results on lipids with both chains being unsaturated may not be comparable with previous studies. Another feature of simulated transbilayer pressure profiles are increased values in the chain segments close to the phospholipid headgroups, which were not present in our NMR based analysis. These high values in the MD simulations may actually reflect partially the transbilayer pressure exerted by the headgroups, as the mobility of the lipid molecules in the simulation leads to a time-dependent localization of headgroups in the chain region and vice versa, and blurs the transbilayer pressure profile. In our analysis, however, this dynamic aspect was not considered and the transbilayer pressure profile presents exclusively the contribution from the acyl chains. Considering the NMR data, we obtained a good agreement with studies of DOPC [45]. Data of lipids with more than one double bond in both chains has not been acquired previously to our knowledge.

We found that MscL and MscS, which have served over many years as models of MS ion channels gated by bilayer tension according to the "force-from-lipids" principle [23], [46], including TREK1, TREK-2 [47], TRAAK and Piezo1[48], [49], [50], [51], [52], [53], respond differently to poly-unsaturated lipids. Whilst the opening/closing behavior of MscL is mostly dominated by the reduction of membrane thickness accompanying increasing number of double bonds (**Fig.5A**), MscS mainly responds to the distribution of the transbilayer pressure across the bilayer (**Fig. 5B**). Membrane thinning in the case of MscL leads to a reduction of the tension required for channel opening due to decreased hydrophobic mismatch between the open channel state and the bilayer as demonstrated by a study combining EPR spectroscopy and patch clamp recording showing that MscL required less tension for activation in bilayers made of shorter lipids compared to bilayers made of longer lipids [24]. Using NMR, we measured and confirmed a decrease in membrane thickness with increasing unsaturation (**Table 1**), in agreement with previous reports [31], though in our study the thinning effect was found to be more pronounced. A thickness difference of up to 4.5 Å and 5.3 Å in the case of PC and PC/PE between the hydrophobic chain regions of 18:1 and 18:3 bilayers, respectively, was observed. Note that a value of 2.5 Å has been reported in [31]. In our patch clamp experiments, the threshold of activation ratio of open MscL to open MscS for 18:3 lipids, of 1.49, is similar to the respective ratio in thinner 16:1 PE/PC bilayers of 1.39 ± 0.11 reported by Nomura et al. [[22], **SI**]. Interestingly, the data by Nomura et al. [22] also show that the activation threshold of MscL, co-reconstitued with MscS, was reduced by ~27% in thinner 16:1 bilayers compared to 18:1, a value that closely resembles our observed difference in MscL activation threshold between 18:1 and

18:3 bilayers (~24%). Together, these observations support our conclusion that thickness of polyunsaturated bilayers is the main parameter responsible for the PUFAs effect on MscL.

In the MscS case, we observed an increase of the hysteresis between opening and closing phases, and reduction in channel closing rate when reconstituted in poly-unsaturated lipids. As evident from the delayed closing times (**Fig. 2A and 2C**) and reduced number of brief gating events in 18:2 and 18:3 lipids (**Fig. 3**), an increasing number of double bonds in the lipid acyl chains apparently stabilized the open state of the channel. Similar to our findings, MscS was shown to be less sensitive to changes in bilayer thickness but exhibited larger sensitivity to bilayer stiffness compared to MscL [22]. We suggest that the lipid saturation effect on MscS arises mainly from the changes in transbilayer pressure profile of the softer poly-unsaturated bilayer, given our NMR results allowing us to determine experimentally the transbilayer profile of these bilayers. Comparing the shapes of the closed and open MscS conformations [54], [55], a distinct difference can be noticed, which corresponds to the area change occupied by the two conformations of $\Delta A = 7.8$ nm^2 on the periplasmic side of the transmembrane segment and of $\Delta A = 4.6$ nm^2 on the cytoplasmic side [56]. As seen in the shape profiles of MscS in Figure 5C, the closed form of MscS possesses a small diameter on the periplasmatic side, which is expanded in the open form. Hence the closed form does not match the lateral pressure profile of lipids with high degree of unsaturation very well, as then the relatively low pressure at the outer regions of the hydrophobic slab would meet a small protein cross sectional area, whilst the high pressure in the bilayer center meets a larger protein cross sectional area. The open form is better adapted to poly-unsaturated lipids, as the relatively low lateral pressure of the outer membrane regions coincides then with a larger protein cross section. Interestingly, for MscS channel gating by the

"force-from-lipids" a scheme was proposed and called the "jack-in-the-box" gating paradigm where removal or reduction in certain regions of the transbilayer pressure profile allows the channel to 'spring' into the open state [57]. Considering the predicted cross-sectional area changes, the internal tension in MscS making the channel spring open are located near the headgroup region of the bilayer and not in the center of the bilayer. Our NMR experiments revealed that the area/lipid increased with the level of unsaturation in PC/PE bilayers (**Table 1**) used for the patch clamp experiments in this study (**Fig. 3**). This is in line with the finding that the transbilayer pressure profile, where the pressure is focused in the bilayer center and respectively reduced near the apolar/polar interface as in the case of 18:3 lipids, spreads over a larger chain region without double bonds. Hence, we expect that the multiple unsaturated lipids 18:2 and 18:3 should allow the internal tension within MscS to relax easier and thus stabilize the open state of MscS, which is indeed what we observed in the patch clamp experiments. Furthermore, it has been suggested that tension sensing by MscS involves lipids intruding into the channel pockets formed between the transmembrane helices [54]. Even if lipids are present in these hydrophobic pockets preventing the gating transition they are likely to exert direct force on the channel elements [58]. Consequently, both entropy-driven "jack-in-the-box" MscS opening as well as lipid pulling from the pockets seems required to fully explain the MscS channel gating as indicated by our study.

Furthermore, a critical structural difference between MscS and MscL is the size of the open channel pore formed by five TM1 transmembrane helices in MscL and 7 TM3 transmembrane helices in MscS. In the case of the MscL pentamer, the opening of the very large channel pore of 30 Å in diameter is achieved by a significant tilt of the TM1 and TM2 transmembrane helices

resulting in the reduction of the thickness of the transmembrane portion of the channel following the reduction of the lipid bilayer thickness [22, 24]. In the case of the MscS heptamer, a lesser tilt of the TM1 and TM2 helices is required to accommodate the smaller MscS open channel pore of 14–16 Å [22, 56].

The presence of both MS channels in 18:3 bilayers reduces the magnitude of the observed effects on mono-reconstituted channels in the same lipid environment (**Fig. 5C**). MscL sensitivity and MscS hysteresis are both reduced when both channels are present in poly-unsaturated bilayers. These very distinct behaviors can be explained by the conformational changes and changes in the transbilayer pressure profile in the proteins upon opening/closing. The transmembrane domain of MscL is predicted to increase in the mid-bilayer cross section more than at its boundaries upon opening but its opening is facilitated, rather than opposed, by the higher pressure in the bilayer core. However, MscL also decreases in its hydrophobic thickness upon opening; hence hydrophobic mismatch seems to be the dominant driving force for its observed response to lipid saturation as we already concluded from experiments with mono-reconstituted MscL. MscS on the other hand changes from a conical shape to an hourglass profile with a constriction in the center of the membrane when opening. Furthermore, when MscL was mono-reconstituted into 18:3 bilayers its activation threshold was reduced by ~42% compared to its threshold in 18:1 bilayers (**Fig. 2D**). When MscS and MscL were co-reconstituted (**Fig. 2E**), the opening threshold of MscL was reduced by only ~24% in 18:3 compared to 18:1. This difference between reconstitution of MscL alone vs co-reconstitution with MscS possibly results from clustering of the two channel species since clustering could reduce the hydrophobic mismatch between the closed MscL channel and the bilayer due to contact with MscS [22]. Clustering was reported to

increase the activation thresholds of both MS channels [22]. In 18:3 bilayers, neighboring MscS may compensate for the hydrophobic mismatch experienced by MscL leading to an increase of the activation threshold of the latter. In turn, clustering causes MscS to close earlier and reduces its closing hysteresis (Fig. 5C). These findings are consistent with the recent molecular modelling studies showing that membrane proteins modulate their local lipid environment and functionally depend closely on their local lipid composition [1], and protein-protein interactions [22].

In light of the results described in our study it will be important to investigate how other mechanosensitive channels, such as TREK-1, TREK-2 [47] and TRAAK [50], as well as Piezo1[52], [53] and Piezo2 channels are modulated by lipid saturation and whether the MscS/MscL paradigm applies to them as well.

SUMMARY

Mechanosensitive channels MscL and MscS are differentially modulated by poly-unsaturated fatty acids in lipid bilayers. MscL becomes sensitized because of increased hydrophobic mismatch while MscS open state is stabilized due to changes in the bilayer lateral pressure profile determined by NMR.

References

[1] Corradi V, Mendez-Villuendas E, Ingolfsson H, Marrink SJ, Tieleman DP. Lipid-Protein Interactions are Unique Fingerprints for Membrane Proteins. Biophysical journal. 2017;112: 84a.

[2] Lehninger AL, Nelson DL, Cox MM. Lehninger principles of biochemistry. 4th ed. New York: W.H. Freeman; 2005.
[3] Andersen OS, Koeppe RE, 2nd. Bilayer thickness and membrane protein function: an energetic perspective. Annual review of biophysics and biomolecular structure. 2007;36:107-30.
[4] Levitan I, Fang Y, Rosenhouse-Dantsker A, Romanenko V. Cholesterol and Ion Channels. Subcell Biochem. 2010;51:509-49.
[5] Anishkin A, Kung C. Stiffened lipid platforms at molecular force foci. Proceedings of the National Academy of Sciences of the United States of America. 2013;110:4886-92.
[6] Qi Y, Andolfi L, Frattini F, Mayer F, Lazzarino M, Hu J. Membrane stiffening by STOML3 facilitates mechanosensation in sensory neurons. Nature communications. 2015;6:8512.
[7] Turk HF, Chapkin RS. Membrane lipid raft organization is uniquely modified by n-3 polyunsaturated fatty acids. Prostaglandins, leukotrienes, and essential fatty acids. 2013;88:43-7.
[8] Vasquez V, Krieg M, Lockhead D, Goodman MB. Phospholipids that contain polyunsaturated fatty acids enhance neuronal cell mechanics and touch sensation. Cell reports. 2014;6:70-80.
[9] Ye S, Tan L, Ma J, Shi Q, Li J. Polyunsaturated docosahexaenoic acid suppresses oxidative stress induced endothelial cell calcium influx by altering lipid composition in membrane caveolar rafts. Prostaglandins, leukotrienes, and essential fatty acids. 2010;83:37-43.
[10] Randall AS, Liu CH, Chu B, Zhang Q, Dongre SA, Juusola M, et al. Speed and sensitivity of phototransduction in Drosophila depend on degree of saturation of membrane phospholipids. The Journal of neuroscience : the official journal of the Society for Neuroscience. 2015;35:2731-46.
[11] Volmer R, Ron D. Lipid-dependent regulation of the unfolded protein response. Current opinion in cell biology. 2015;33:67-73.
[12] Gawrisch K, Soubias O, Mihailescu M. Insights from biophysical studies on the role of polyunsaturated fatty acids for function of G-protein coupled membrane receptors. Prostaglandins, leukotrienes, and essential fatty acids. 2008;79:131-4.
[13] Schumann J. It is all about fluidity: Fatty acids and macrophage phagocytosis. European journal of pharmacology. 2015.
[14] Siscovick DS, Lemaitre RN, Mozaffarian D. The fish story: a diet-heart hypothesis with clinical implications: n-3 polyunsaturated fatty acids, myocardial vulnerability, and sudden death. Circulation. 2003;107:2632-4.
[15] Jung UJ, Torrejon C, Tighe AP, Deckelbaum RJ. n-3 Fatty acids and cardiovascular disease: mechanisms underlying beneficial effects. The American journal of clinical nutrition. 2008;87:2003S-9S.
[16] Mazza M, Pomponi M, Janiri L, Bria P, Mazza S. Omega-3 fatty acids and antioxidants in neurological and psychiatric diseases: an overview. Progress in neuro-psychopharmacology & biological psychiatry. 2007;31:12-26.
[17] Yang X, Sheng W, Sun GY, Lee JC. Effects of fatty acid unsaturation numbers on membrane fluidity and alpha-secretase-dependent amyloid precursor protein processing. Neurochemistry international. 2011;58:321-9.
[18] Noel J, Sandoz G, Lesage F. Molecular regulations governing TREK and TRAAK channel functions. Channels. 2011;5:402-9.
[19] Kloda A, Lua L, Hall R, Adams DJ, Martinac B. Liposome reconstitution and modulation of recombinant N-methyl-D-aspartate receptor channels by membrane stretch. Proceedings of the National Academy of Sciences of the United States of America. 2007;104:1540-5.

[20] Nagao K, Yanagita T. Medium-chain fatty acids: functional lipids for the prevention and treatment of the metabolic syndrome. Pharmacological research. 2010;61:208-12.
[21] Vara-Messler M, Buccellati C, Pustina L, Folco G, Rovati GE, Hoxha M. A potential role of PUFAs and COXIBs in cancer chemoprevention. Prostaglandins & other lipid mediators. 2015;120:97-102.
[22] Nomura T, Cranfield CG, Deplazes E, Owen DM, Macmillan A, Battle AR, et al. Differential effects of lipids and lyso-lipids on the mechanosensitivity of the mechanosensitive channels MscL and MscS. Proceedings of the National Academy of Sciences of the United States of America. 2012;109:8770-5.
[23] Martinac B, Adler J, Kung C. Mechanosensitive ion channels of E. coli activated by amphipaths. Nature. 1990;348:261-3.
[24] Perozo E, Kloda A, Cortes DM, Martinac B. Physical principles underlying the transduction of bilayer deformation forces during mechanosensitive channel gating. Nature structural biology. 2002;9:696-703.
[25] Häse CC, Le Dain AC, Martinac B. Purification and functional reconstitution of the recombinant large mechanosensitive ion channel (MscL) of Escherichia coli. The Journal of biological chemistry. 1995;270:18329-34.
[26] Ridone P, Nakayama Y, Martinac B, Battle AR. Patch clamp characterization of the effect of cardiolipin on MscS of E. coli. European biophysics journal : EBJ. 2015;44:567-76.
[27] Colquhoun D. Practical analysis of single channel records.
[28] Nevzorov AA, Opella SJ. Selective averaging for high-resolution solid-state NMR spectroscopy of aligned samples. J Magn Reson. 2007;185:59-70.
[29] Nagle JF. Area Lipid of Bilayers from Nmr. Biophysical journal. 1993;64:1476-81.
[30] Grage SL, Afonin S, Kara S, Buth G, Ulrich AS. Membrane Thinning and Thickening Induced by Membrane-Active Amphipathic Peptides. Frontiers in cell and developmental biology. 2016;4:65.
[31] Rawicz W, Olbrich KC, McIntosh T, Needham D, Evans E. Effect of chain length and unsaturation on elasticity of lipid bilayers. Biophysical journal. 2000;79:328-39.
[32] Delcour AH, Martinac B, Adler J, Kung C. Modified reconstitution method used in patch-clamp studies of Escherichia coli ion channels. Biophysical journal. 1989;56:631-6.
[33] de Planque MRR, Greathouse DV, Koeppe RE, Schafer H, Marsh D, Killian JA. Influence of lipid/peptide hydrophobic mismatch on the thickness of diacylphosphatidylcholine bilayers. A H-2 NMR and ESR study using designed transmembrane alpha-helical peptides and gramicidin A. Biochemistry. 1998;37:9333-45.
[34] Holte LL, Peter SA, Sinnwell TM, Gawrisch K. 2H nuclear magnetic resonance order parameter profiles suggest a change of molecular shape for phosphatidylcholines containing a polyunsaturated acyl chain. Biophysical journal. 1995;68:2396-403.
[35] Shaikh SR, Kinnun JJ, Leng XL, Williams JA, Wassall SR. How polyunsaturated fatty acids modify molecular organization in membranes: Insight from NMR studies of model systems. Bba-Biomembranes. 2015;1848:211-9.
[36] Cantor RS. Lipid composition and the lateral pressure profile in bilayers. Biophysical journal. 1999;76:2625-39.
[37] Marsh D. Lateral pressure profile, spontaneous curvature frustration, and the incorporation and conformation of proteins in membranes. Biophysical journal. 2007;93:3884-99.
[38] Gullingsrud J, Schulten K. Lipid bilayer pressure profiles and mechanosensitive channel gating. Biophysical journal. 2004;86:3496-509.

[39] Feller SE, Gawrisch K, MacKerell AD. Polyunsaturated fatty acids in lipid bilayers: Intrinsic and environmental contributions to their unique physical properties. J Am Chem Soc. 2002;124:318-26.
[40] Law JMS, Szori M, Izsak R, Penke B, Csizmadia IG, Viskolcz B. Folded and unfolded conformations of the omega-3 polyunsaturated fatty acid family: CH3CH2[CH=CHCH2](B)[CH2](M)COOH. First principles study. J Phys Chem A. 2006;110:6100-11.
[41] Templer RH, Castle SJ, Curran AR, Rumbles G, Klug DR. Sensing isothermal changes in the lateral pressure in model membranes using di-pyrenyl phosphatidylcholine. Faraday Discuss. 1998;111:41-53.
[42] Gawrisch K, Holte LL. NMR investigations of non-lamellar phase promoters in the lamellar phase state. Chemistry and physics of lipids. 1996;81:105-16.
[43] Carrillo-Tripp M, Feller SE. Evidence for a mechanism by which omega-3 polyunsaturated lipids may affect membrane protein function. Biochemistry. 2005;44:10164-9.
[44] Ollila S, Hyvonen MT, Vattulainen I. Polyunsaturation in lipid membranes: dynamic properties and lateral pressure profiles. The journal of physical chemistry B. 2007;111:3139-50.
[45] Warschawski DE, Devaux PF. Order parameters of unsaturated phospholipids in membranes and the effect of cholesterol: a H-1-C-13 solid-state NMR study at natural abundance. Eur Biophys J Biophy. 2005;34:987-96.
[46] Teng J, Loukin S, Anishkin A, Kung C. The force-from-lipid (FFL) principle of mechanosensitivity, at large and in elements. Pflugers Archiv : European journal of physiology. 2015;467:27-37.
[47] Clausen MV, Jarerattanachat V, Carpenter EP, Sansom MSP, Tucker SJ. Asymmetric mechanosensitivity in a eukaryotic ion channel. Proceedings of the National Academy of Sciences of the United States of America. 2017.
[48] Brohawn SG, Su ZW, Mackinnon R. Mechanosensitivity is mediated directly by the lipid membrane in TRAAK and TREK1 K+ channels. Proceedings of the National Academy of Sciences of the United States of America. 2014;111:3614-9.
[49] Brohawn SG, Campbell EB, MacKinnon R. Physical mechanism for gating and mechanosensitivity of the human TRAAK K+ channel. Nature. 2014;516:126-30.
[50] Berrier C, Pozza A, de Lacroix de Lavalette A, Chardonnet S, Mesneau A, Jaxel C, et al. The purified mechanosensitive channel TREK-1 is directly sensitive to membrane tension. The Journal of biological chemistry. 2013;288:27307-14.
[51] Dong YY, Pike AC, Mackenzie A, McClenaghan C, Aryal P, Dong L, et al. K2P channel gating mechanisms revealed by structures of TREK-2 and a complex with Prozac. Science. 2015;347:1256-9.
[52] Syeda R, Florendo MN, Cox CD, Kefauver JM, Santos JS, Martinac B, et al. Piezo1 Channels Are Inherently Mechanosensitive. Cell reports. 2016;17:1739-46.
[53] Cox CD, Bae C, Ziegler L, Hartley S, Nikolova-Krstevski V, Rohde PR, et al. Removal of the mechanoprotective influence of the cytoskeleton reveals PIEZO1 is gated by bilayer tension. Nature communications. 2016;7.
[54] Pliotas C, Dahl AC, Rasmussen T, Mahendran KR, Smith TK, Marius P, et al. The role of lipids in mechanosensation. Nature structural & molecular biology. 2015;22:991-8.
[55] Steinbacher S, Bass R, Strop P, Rees DC. Structures of the prokaryotic mechanosensitive channels MscL and MscS. Curr Top Membr. 2007;58:1-24.

[56] Shaikh S, Cox CD, Nomura T, Martinac B. Energetics of gating MscS by membrane tension in azolectin liposomes and giant spheroplasts. Channels. 2014;8:321-6.
[57] Malcolm HR, Blount P, Maurer JA. The mechanosensitive channel of small conductance (MscS) functions as a Jack-In-The Box. Bba-Biomembranes. 2015;1848:159-66.
[58] Bavi N, Cox CD, Perozo E, Martinac B. Toward a structural blueprint for bilayer-mediated channel mechanosensitivity. Channels. 2017;11:91-3.

FIGURE LEGENDS

Figure 1. MscS and MscL are gated by tension propagated through the bilayer. Force-from-lipids is modulated by inter-lipid attractive and repulsive interactions [31]. The inset schematically shows the contribution of each of these forces to the transbilayer pressure profile of the bilayer from the perspective of four neighboring DOPC molecules. The estimated tension magnitudes required to open MscS and MscL are reported below the red arrows (T stands for tension). MscS and MscL monomers are also highlighted.

Figure 2. Effect of lipid saturation on the gating of MscS and MscL. (A) MscS response to a 0-60 mmHg ramp in 18:1 (black) and 18:3 (red) liposomes. The red trace shows a delay in MscS closing. (B) MscL response to a 0-60 mmHg ramp in 18:1 (black) and 18:3 (red) liposomes.

MscL thresholds are significantly reduced in 18:3 lipids. (C) Co-reconstituted MscS and MscL response to a 0-80 mmHg ramp in 18:1 liposomes (black) and a 0-50 mmHg ramp in 18:3 liposomes (red); arrows indicate MscS opening, MscL opening, MscL closing and MscS closing (left to right) for 18:1 (black) and 18:3 (red). Summary of the first-opening and the last-closing event thresholds (mmHg) for single reconstituted channels (D: MscS in 18:1 (n=7), MscS in 18:3 (n=3), MscL in 18:1 (n=7), MscL in 18:3 (n=5)) and co-reconstituted channels (E: 18:1 lipid (n=31), 18:2 (n=8), 18:3 (n=26)). Boltzmann curves of MscL (F, G) and MscS (H, I) mechanosensitivity during the opening (F & H) and closing (G & I) regimes, in different lipid environments. Error bars represent standard error. P-values were calculated with 1-way ANOVA (Fig.2D) and 2-way ANOVA (Fig.2E).
[* = $p < 0.05$, ** = $p < 0.005$, *** = $p < 0.0005$].

Figure 3. MscS gating frequency is reduced in poly-unsaturated bilayers. The current recordings show a population of MscS opening in response to similar, ascending, pressure ramps in (A) 18:1 lipids (22 channels), (B) 18:2 lipids (27 channels) and (C) 18:3 lipids (40 channels). The 'flickery' gating for each experimental sample is quantified in the histogram shown in (D). The insets in (A),(B) and (C) show the structure of mono- and poly-unsaturated (all-cis) PC lipids and a magnified portion of the trace above the red line (100ms interval), where the amplitude of a single MscS is highlighted in blue (30 pA)P-values were obtained via Student's t-test (**** = $p < 0.00005$). Each N represents a single recording from different patches. Each experimental replicate was obtained from an average number of channels per patch of 29 (18:1), 20 (18:2) and 10 (18:3). Error bars represent Standard Error.

Figure 4. Trans-bilayer lateral pressure profile of the hydrophobic core. (A, B) Lipid order parameter of PC and PC:PE bilayers respectively. Black arrows highlight the carbons flanking a C=C double bond. Legend: Black: 18:1; Grey: 18:2 ; White: 18:3. (C, D) Change in membrane thickness derived from lipid order parameters of PC and PC:PE bilayers respectively. Black arrows highlight the carbons flanking a C=C double bond. Legend: Black: 18:1; Grey: 18:2 ; White: 18:3. (E, F) Lateral pressure profile of the hydrophobic core (carbon 3, to carbon 18 of the acyl chain) with respect to its thickness (Å), for PC and PC:PE bilayers, respectively. Error bars represent standard error of the mean.

Figure 5. Differential effect of PUFAs on MscS and MscL. A) Vertical section of the MscL transmembrane domain embedded in 18:1 (left) and 18:3lipids (right). The 18:3 lipid disordered hydrophobic core is thinner than in 18:1, thus increasing the sensitivity of MscL embedded therein. Bilayer thickness values taken from [31]. B) Lipid unsaturation doesn't affect the sensitivity of MscS (left) during the opening phase, while it delays its closing phase due to the increased internal pressure at the hydrophobic core. A schematic transbilayer pressure profile for each bilayer type is shown to highlight the differential pressure exerted on the periphery of the MscS channel transmembrane domain (solid line for 18:1, dashed line for 18:3). C) In 18:3 lipids, clustering of MscS and MscL attenuates the effects observed when the channels are reconstituted singularly. Protein-lipid and protein-protein interactions both participate in the functional modulation of MS channel activity.

Table 1. Bilayer parameters determined from NMR experiments.

acyl chain	PC hydrophobic thickness (Å)	integral transbilayer pressure (mN/m)	area/lipid (Å^2)	PC:PE (2:1) hydrophobic thickness (Å)	integral transbilayer pressure (mN/m)	area/lipid (Å^2)
18:1	24.9 ± 0.1	11.5 ± 0.6	65.2 ± 0.5	25.1 ± 0.1	11.3 ± 0.6	64.8 ± 0.5
18:2	22.4 ± 0.1	14.0 ± 0.6	65.5 ± 0.5	21.2 ± 0.1	12.9 ± 0.8	67.9 ± 0.5
18:3	20.4 ± 0.1	14.0 ± 1.0	66.1 ± 0.5	19.7 ± 0.1	10.9 ± 0.9	71.5 ± 0.5

Thickness of the hydrophobic portion of the bilayers made of mono- and polyunsaturated PC and PC/PE lipids estimated from the order parameter determined by NMR. Integrated transbilayer pressures of the hydrophobic core of the bilayers and area/lipid of lipids with different head-groups and degree of unsaturation were also obtained from NMR experiments. PC = 1,2-dioleoyl-sn-glycero-3- phosphocholine, PE = 1,2-dioleoyl-sn-glycero-3-phosphoethanolamine.

Fig.5

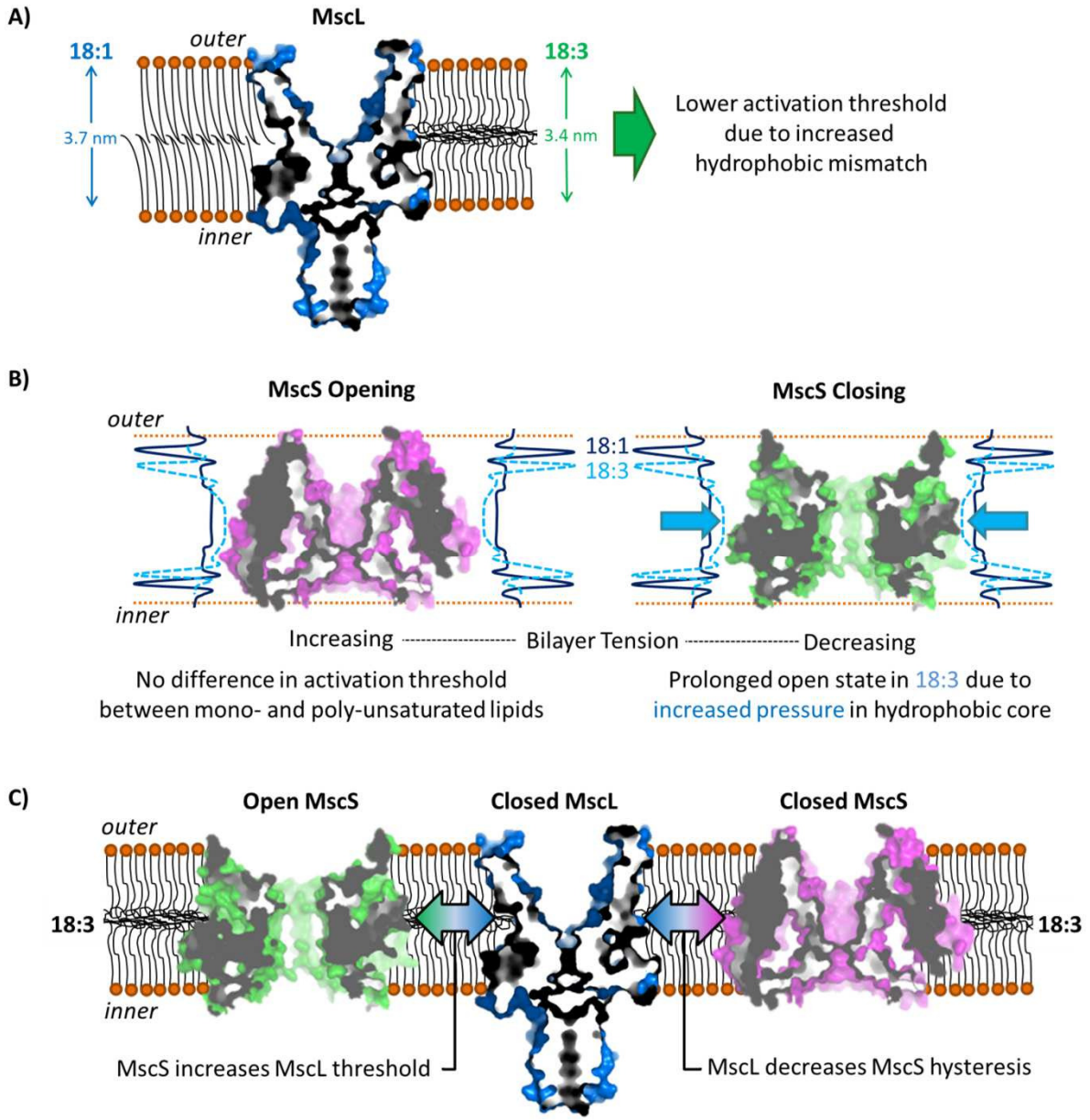

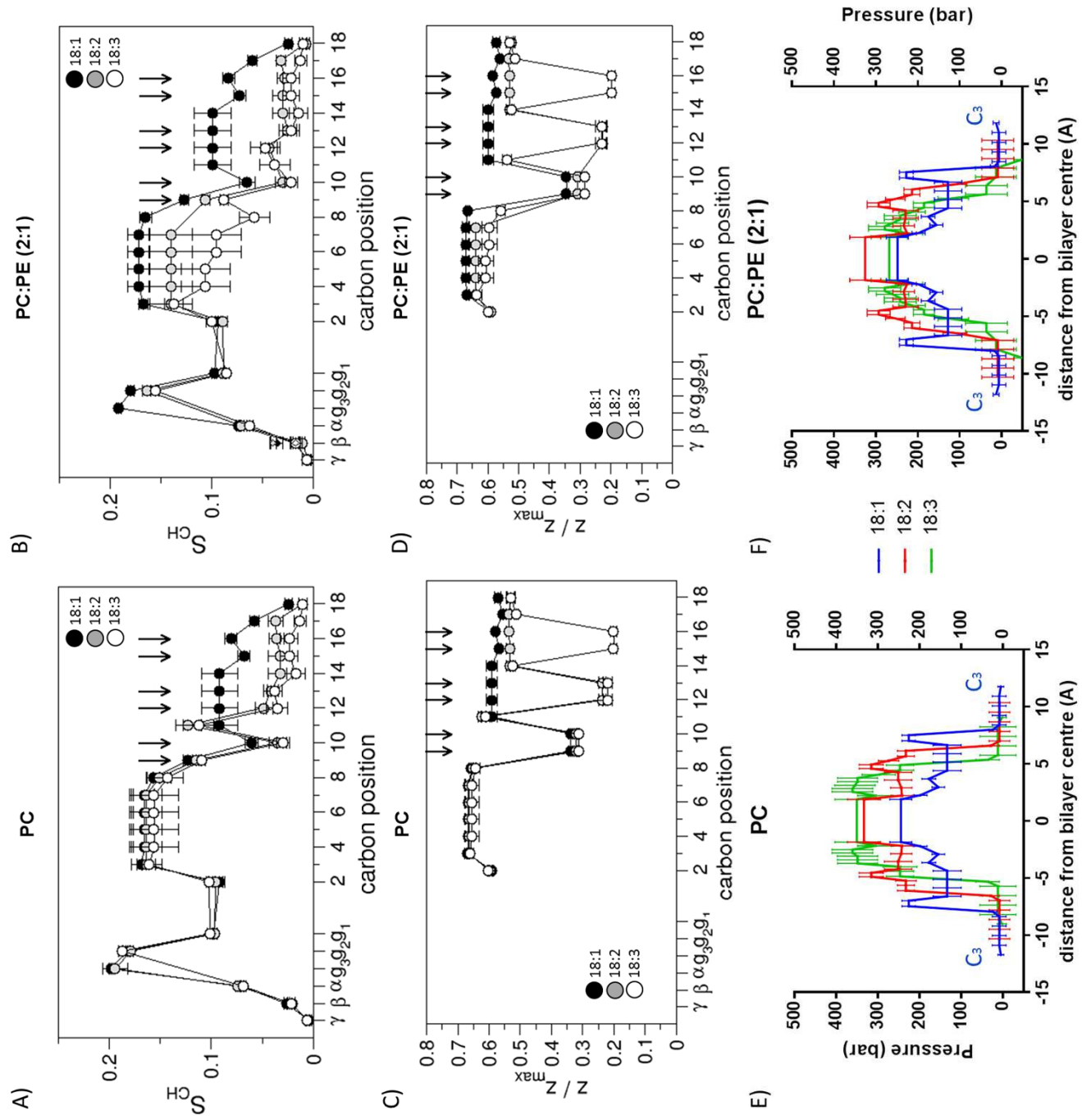

Fig.4

Fig.3

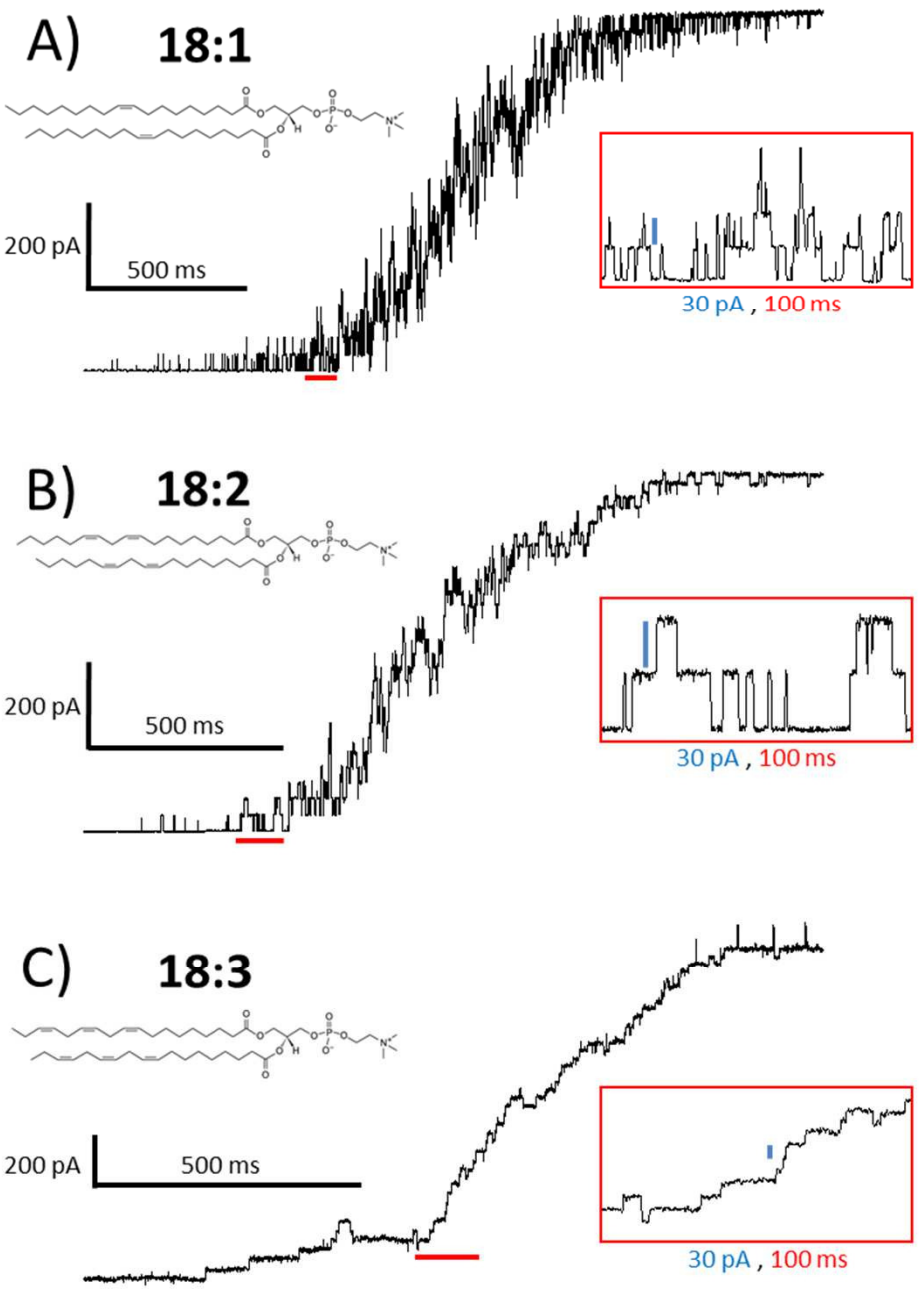

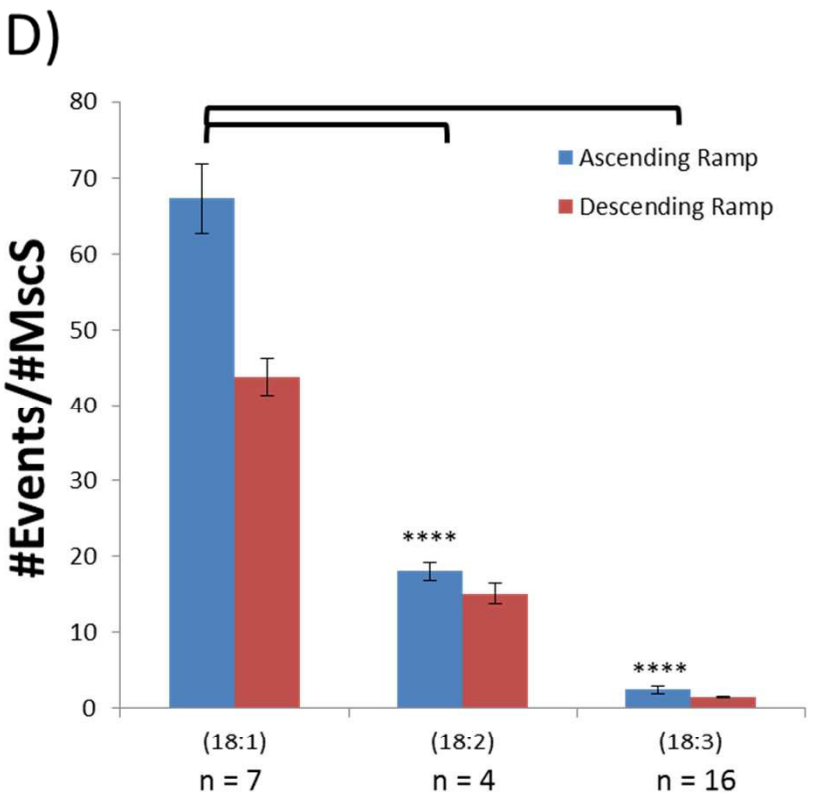

Fig.2

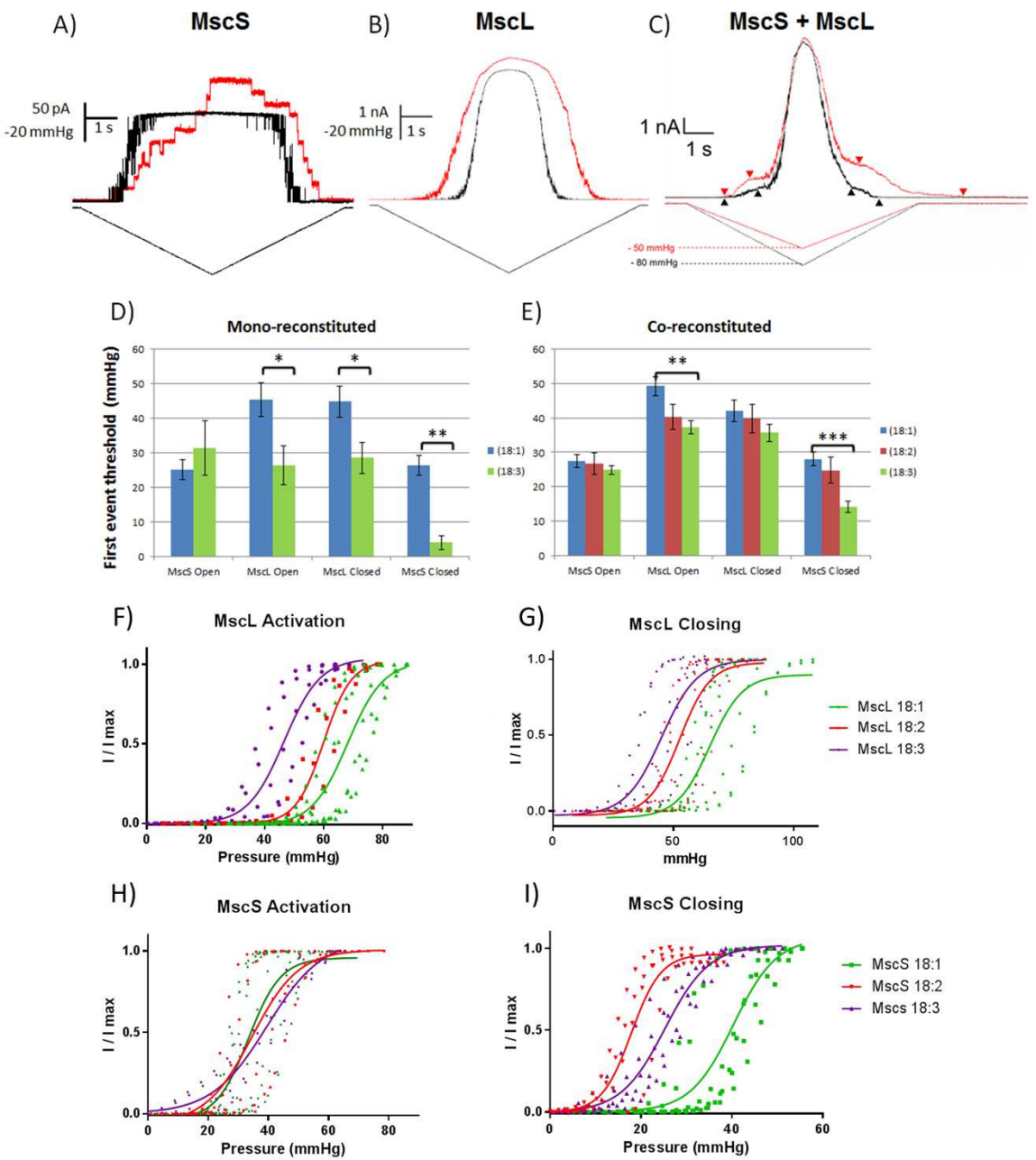

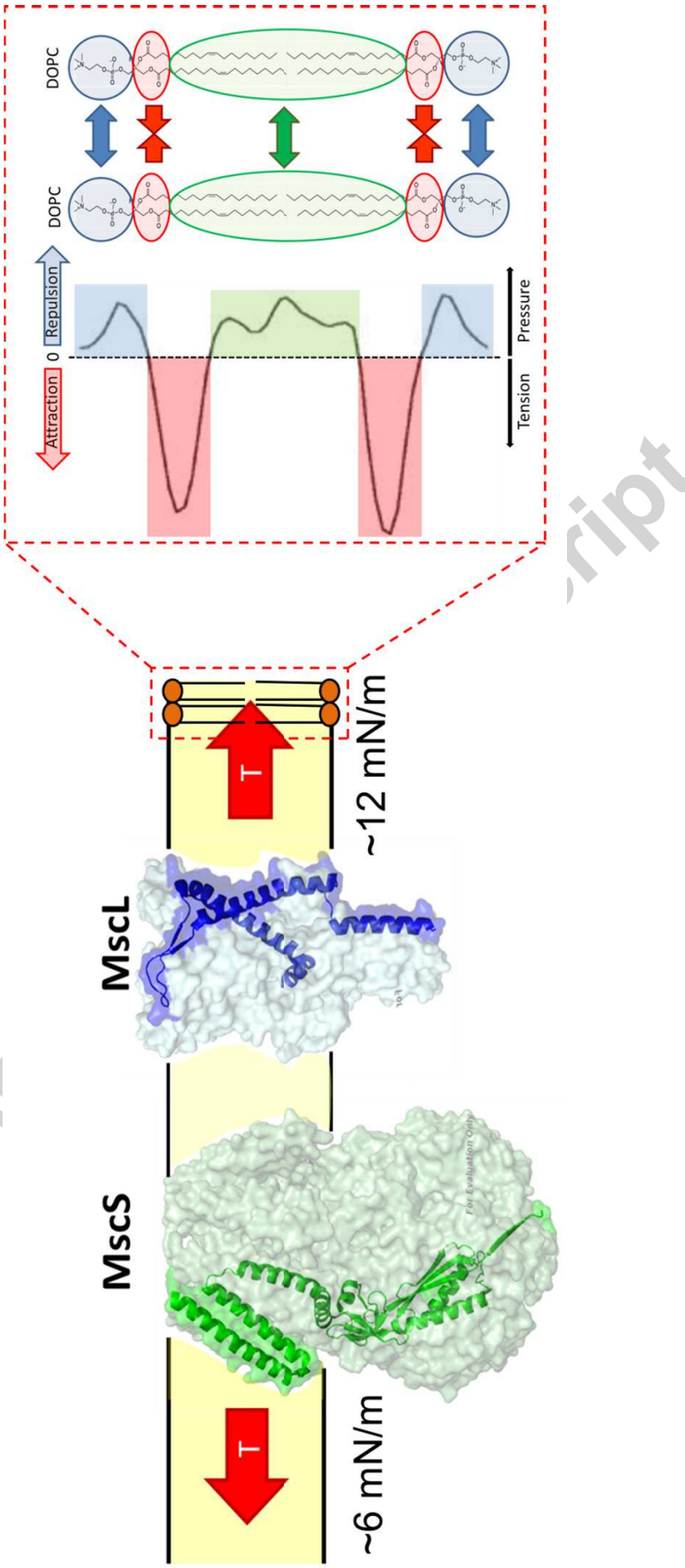
DOPC
DOPC
Repulsion
0
Attraction
Pressure
Tension
T
~12 mN/m
MscL
MscS
T
~6 mN/m

Fig.1